CLM - P 69

United Kingdom Atomic Energy Authority

RESEARCH GROUP

Preprint

A CONTROL ENGINEERING APPROACH TO MAGNETOHYDRODYNAMIC STABILITY

W. H. B. COOPER
A. B. GILLESPIE
E. E. ALDRIDGE
J. CONTOS

Culham Laboratory,

Culham, Abingdon, Berkshire

1965

UNCLASSIFIED
(Approved for publication)

CLM - P69

A CONTROL ENGINEERING APPROACH TO MAGNETOHYDRODYNAMIC STABILITY

by

W.H.B. COOPER+
A.B. GILLESPIE+
E.E. ALDRIDGE+
J. CONTOS*

(Submitted for publication in Proc. Instn. Elec. Engrs.)

+United Kingdom Atomic Energy Authority, Electronics Division, Atomic Energy Research Establishment, Harwell.

*Nuclear Research Centre "Democritus" Athens. Dr. Contos co-operated in this work while attached to the Electronics Division, Atomic Energy Research Establishment, Harwell during the last year of his Ph.D. studies in the Electrical Engineering Department of Birmingham University.

U.K.A.E.A. Research Group,
Culham Laboratory,
Nr. Abingdon,
Berks.

July, 1965. (C/18 MEA)

ABSTRACT

The well-established transfer function method of determining the stability of lumped parameter dynamic systems is applied in the paper to a study of the stability of an infinitely conducting fluid immersed in a magnetic field.

Such a system is both distributed in space and multi-dimensional and it is shown how, by the application of a modal energisation technique, the whole may be replaced by a number of simpler systems, each subjected to a spatial energisation in the fundamental or a higher order (harmonic) mode and each amenable to a one-dimensional analytical treatment. Complete stability is obtained only if all the component systems are themselves individually stable.

To accommodate the distributed nature of the system the concept of field impedance is introduced, and to help the electrical engineer to understand and appreciate better the physical significance of the problem the whole is converted to an equivalent circuit or analogue, involving electrical transmission lines. A further advantage of this approach is, of course, the wealth of analytical solutions and tabulated transforms which are applicable to the electrical network field.

Two particular geometrical configurations are then discussed in detail. In the first, a cylindrical fluid is contained by an axially directed magnetic field and in the second, a cylindrical fluid is contained by a circumferentially directed magnetic field. These are two geometries which have been intensively studied in the controlled thermonuclear fusion field and are usually referred to as the θ-pinch and the Z-pinch respectively.

C O N T E N T S

1. INTRODUCTION

The practical application of electromagnetic theory increased so spectacularly in the microwave field between 1940 and 1950 that a new approach became necessary. The old practice of working out each boundary value problem as it if were a new one was largely abandoned as repetitive and uneconomical because if failed to co-ordinate the various results. The central theme of the newer approach was the concept of field impedance[1,2].

Also, during the following decade the need for a more unified approach to the understanding of closed loop lumped-parameter dynamical systems led to a more widespread use of transfer functions and transforms as design tools[3,4,5].

This paper is an application of these engineering concepts to magnetohydrodynamics, i.e. the dynamics of ideal conducting fluids. Such an approach will not yield analytical solutions which cannot be obtained by classical methods but for some it will provide an intuitively clearer picture.

There are obvious limitations because superposition principles lie at the root of the concepts of both field impedance and the transforms. The field equations of electromagnetism are linear, whilst the field equations of hydrodynamics are non-linear due, in the first place, to the presence of, and the ideas behind, the transport operator; also when an electromagnetic field penetrates a conducting fluid the combined system is essentially non-linear, due to the coupling mechanism, i.e. the presence of the motor and dynamo terms. This paper, however, is concerned with the formulation of the magnetohydrodynamics in a form which is linearised on the one hand by the assumption of an infinitely high conductivity fluid which prevents penetration of the electromagnetic field and, on the other, by considering perturbations about a set of equilibrium conditions[6].

2. THE MASS-SPRING MODEL

The stability of an infinitely conducting fluid in the presence of external electromagnetic fields can be likened to the simple mass-spring model of Fig.1 so

closely that the behaviour of the latter is worth recounting in detail. In developing the analogy analytically it is conceptually useful to consider the mass-spring model flow diagram as a closed loop system expressed in terms of force F and velocity u as dependent variables; the fluid counterparts are pressure and velocity.

Initially, the system is postulated to be in static equilibrium where the weight of the mass M is balanced by the tension of the spring. Suppose now the system is perturbed by the application of an external force F_e. At some time t later the mass will be displaced a distance x and if the proportionality factor of the spring is K we have:

Spring restoring force $$F_r = Kx$$

$$\equiv K \int u\,dt$$

$$= K \frac{u}{s} \qquad \ldots (1)$$

where $$\frac{1}{s} = \int dt$$

Accelerating force $$F_a = M \frac{d^2x}{dt^2}$$

$$= M \frac{du}{dt}$$

$$= Msu \qquad \ldots (2)$$

where $$s = \frac{d}{dt}$$

and the system configuration is defined by

$$F_e - F_r = F_a \qquad \ldots (3)$$

Equation (1) may be rewritten as:

$$F_r = Z_n u \qquad \ldots (4)$$

where Z_n is referred to as the impedance of the spring.

Likewise equation (2) may be rewritten as

$$F_a = Z_m u \qquad \ldots (5)$$

where Z_m is referred to as the impedance of the mass.

Equations (3), (4) and (5) are depicted in conventional seromechanical lang-usage in Fig.2(a). The object of this paper is to express the hydrodynamic and electromagnetic field behaviour in a similar kind of language.

The system transfer function connecting the response u with the applied force F_e is

$$\frac{\frac{1}{Z_m}}{1 - (\frac{1}{Z_m})\ (-\ Z_n)} = \frac{1}{Z_m + Z_n} .$$

In terms of the system parameters this is $\frac{1}{K}\ \frac{\frac{K}{M}\ s}{(s^2 + \frac{K}{M})}$,

and the velocity response to say a unit step of applied force will be

$$\frac{1}{K}\ \text{Sin}\ \sqrt{\frac{K}{M}}\ t .$$

This is illustrated in Fig.2(b) and the system is neutrally stable.

Consider now the case where the spring constant K becomes negative, i.e. a de-restoring force. This mechanical situation has many counterparts operating in terms of angular rather than linear displacements, e.g. a weather vane pivoted to leeward of its centre of pressure or an aircraft with its centre of pressure ahead of its centre of gravity.

The system transfer function becomes

$$\frac{1}{K}\ \frac{\frac{K}{M}\ s}{(s^2 - \frac{K}{M})} ,$$

giving a step response of

$$\frac{1}{K}\ \text{Sinh}\ \sqrt{\frac{K}{M}}\ t .$$

This is shown in Fig.2(c) and the system is now unstable.

An alternative and well-established approach to determining the stability of the system is worth re-stating here. If A(s) is the open loop transfer function

(in this case $A(s) = -\frac{Z_n}{Z_m} = -\frac{K}{s^2M}$) then the characteristic equation of the system is $1 - A(s) = 0$ and the stability depends on the roots of this equation, being unstable if any root has a positive real part. If numerical values of the parameters are available the well-known Nyquist diagram approach may also be useful.

The characteristic equation $1 - A(s) = 0$ is sometimes called the dispersion relationship. In Fig.2(a) an input force F_e was shown for the sake of completeness, but the stability of a linear system is not a function of the stimuli and in later parts of the paper this input will usually be omitted.

3. STABILITY OF THE SIMPLE θ-PINCH CONFIGURATION

This section considers the stability of a cylinder of infinitely conducting fluid surrounded by a vacuum containing a steady uniform axial magnetic field enclosed within an infinitely conducting metal wall. This configuration is approximately produced in a θ-pinch plasma experiment after the pinch or collapse phase is complete. The latter is usually brought about and maintained by a θ-directed current driven around the infinitely conducting metal wall by an external power supply. This fluid, magnetic field geometry, shown in Fig.3, has been chosen as a starting point because its dynamic behaviour can be directly related to that of the mass-spring model. Attention will be confined to a two-dimensional model with variations along the axis and the radius only.

3.1 The Closed Loop Flow Diagram

Since the fluid is infinitely conducting, the steady uniform axial magnetic field H_{oz} is excluded from the interior of the fluid and of necessity a sheet current of density $-J_{o\theta}$ $(= H_{oz})$ flows on the surface of the fluid perpendicular to the axis. Initially, the system is postulated to be in static equilibrium where the pressure P_o within the fluid is balanced by the magnetic pressure $\frac{\mu H_{oz}^2}{2}$ outside.

Suppose the surface of the fluid is perturbed and moves sinusoidally about its equilibrium position with a radial component of velocity u_r and an axial component of velocity u_z. The former is related to the fluctuating pressure p at the surface by $-u_r = \frac{p}{{}_rZ_a^-}$ where ${}_rZ_a^-$ is known as the acoustic field impedance looking radially into the fluid. The negative sign arises because u_r is positive in the direction of increasing radius. Implicit in ${}_rZ_a^-$ is the two-dimensional nature of the problem and its value is thus dependent on boundary conditions in the z direction and on the spatial pattern of the pressure fluctuations, also in the z direction. This aspect of ${}_rZ_a^-$ and likewise of ${}_z^{\theta}Z_e^+$ (see next paragraph) will be discussed in some detail in later sections of the paper.

The fluid surface, moving with a radial velocity u_r then interacts with the steady magnetic field H_{oz} producing an induced fluctuating electric field on the surface (dynamo effect, $u \times \mu H$). Since the fluid is infinitely conducting and thus cannot support a net electric field (i.e. $E + uxB = 0$) this induced electric field must in turn be balanced by an equal and opposite E_θ field. Because of the two-dimensional nature of the problem, this fluctuating E_θ field gives rise to fluctuating magnetic field components H_z and H_r. As before E_θ is related to H_z by $H_z = \frac{E_\theta}{{}_z^{\theta}Z_e^+}$ where ${}_z^{\theta}Z_e^+$ is the electromagnetic field impedance looking radially outwards from the fluid into the vacuum. This corresponds to the propagation of an electromagnetic wave in the radial direction. The value of ${}_z^{\theta}Z_e^+$ is again dependent on the z direction boundary conditions of the system and on the z direction spatial pattern of E_θ, as shown in Section 3.2.

Finally, the steady current $-J_{o\theta}$ flowing on the surface of the fluid reacts with the fluctuating magnetic field H_z producing a surface pressure p (motor effect, $J \times \mu H$) and this completes the loop. The flow diagram of the closed loop is thus as shown in Fig.4 and is similar to that for the mass-spring system in Fig.2(a).

The open loop transfer function is –

$$A(s) = \frac{1}{{}_{r}Z_{a}^{-}} \mu H_{oz} \frac{1}{{}_{z}^{\theta}Z_{e}^{+}} \mu J_{o\theta}$$

$$= \frac{\mu^2 H_{oz} J_{o\theta}}{{}_{r}Z_{a}^{-}\ {}_{z}^{\theta}Z_{e}^{+}} \qquad \ldots (6)$$

$$= - \frac{B_{oz}^2}{{}_{r}Z_{a}^{-}\ {}_{z}^{\theta}Z_{e}^{+}}$$

and the dispersion relationship $1 - A(s) = 0$ becomes

$$1 + \frac{B_{oz}^2}{{}_{r}Z_{a}^{-}\ {}_{z}^{\theta}Z_{e}^{+}} = 0 \qquad \ldots (7)$$

The stability of the system depends on the roots of equation (7) but these cannot be determined until the field impedances ${}_{r}Z_{a}^{-}$ and ${}_{z}^{\theta}Z_{e}^{+}$ have been developed. An established technology exists in the micro-waveguide field for dealing with problems of this kind[1,2] and it will be usefully employed here because of the insight which can be gained when hydromagnetic systems of this kind are thought of in terms of transmission lines.

3.2 The Electromagnetic Field Impedance ${}_{z}^{\theta}Z_{e}^{+}$

Although the simple MHD problem of Section 3.1 has been discussed in cylindrical geometry, there are advantages in introducing the concepts and ideas behind the field impedance approach in Cartesian geometry. An obvious advantage is, of course, mathematical simplicity, but it is also easier to introduce and explain the concept of mode energisation and mode impedance which is a key feature of this approach. If it is assumed that the vacuum outside the fluid is contained in a thin annular space, then without loss of rigour the electromagnetic part of the system can be analysed in Cartesian co-ordinates where E_θ becomes E_y and H_r becomes H_x.

Consider a section through the vacuum, between the fluid and the wall, as shown in Fig.5. The electromagnetic field equations are:

$$\frac{\partial E_y}{\partial z} = j\omega\mu H_x \qquad \ldots (8)$$

$$\frac{\partial E_y}{\partial x} = -j\omega\mu H_z \qquad \ldots (9)$$

and

$$\frac{\partial H_x}{\partial z} - \frac{\partial H_z}{\partial x} = j\omega\varepsilon E_y \qquad \ldots (10)$$

From equations (8) (9) and (10) may be obtained

$$\frac{\partial^2 E_y}{\partial z^2} + \frac{\partial^2 E_y}{\partial x^2} = \Gamma_e^2 E_y \qquad \ldots (11)$$

where

$$\Gamma_e^2 = j\omega\varepsilon j\omega\mu$$

Assume the solution $E_y = E_y(x)\, E_y(z)$ then

$$\frac{1}{E_y(x)} \frac{\partial^2 E_y(x)}{\partial x^2} + \frac{1}{E_y(z)} \frac{\partial^2 E_y(z)}{\partial z^2} = \Gamma_e^2$$

and this is satisfied if

$$\frac{\partial^2 E_y(x)}{\partial x^2} + n^2 E_y(x) = 0 \qquad \ldots (12)$$

and

$$\frac{\partial^2 E_y(z)}{\partial z^2} + k^2 E_y(z) = 0 \qquad \ldots (13)$$

and

$$n^2 + k^2 = -\Gamma_e^2$$

The solution is thus

$$E_y = (A \operatorname{Sin} nx + B \operatorname{Cos} nx)\ (C \operatorname{Sin} kz + D \operatorname{Cos} kz) \qquad \ldots (15)$$

where A B C and D are constants; either n or k is also arbitrary at this stage.

Suppose E_y is assumed zero at $z = +\frac{a}{2}$ and $z = -\frac{a}{2}$ (z direction boundary conditions). This can be satisfied if $C = 0$ and $\operatorname{Cos} \frac{ka}{2} = 0$ giving $\frac{ka}{2} = g\frac{\pi}{2}$ where $g = 1,3,5,7$ ... etc. or alternatively if $D = 0$ and $\operatorname{Sin} \frac{ka}{2} = 0$ giving

$\frac{ka}{2} = g\pi$ where $g = 0,1,2,3 \ldots$ etc. Both are valid solutions, the former giving a cosine distribution about 0, the latter a sine distribution, but only one solution is applicable at any one time.

Each solution for E_y thus consists of the sum of an infinite number of terms having a sinusoidal distribution along the z axis and each term corresponding to one mode (or spatial harmonic) of the possible complex pattern of E_y along z. This is an important concept because in considering the stability of a system like this every mode taken singly must in itself be stable.

Since toroidal configurations are important in pinch discharge work it is interesting at this stage to show how the above analysis can also be applied to a toroid. If E_y is assumed to be symmetrical about 0 this corresponds to a cosine distribution with $C = 0$. If additionally the ends at $z = +\frac{a}{2}$ and $z = -\frac{a}{2}$ are left free then the x distribution of E_y along $z = -\frac{a}{2}$ will be identical with that along $z = -\frac{a}{2}$ and H_x will be zero at all points along the edges. This latter condition is necessary to prevent propagation in the z direction beyond $+\frac{a}{2}$ and $-\frac{a}{2}$. In this case the two edges may be joined together without disturbing the system and this is equivalent to bending the strip round on itself and leads to toroidal geometry in the z direction. To satisfy this condition $\text{Sin}\,\frac{ka}{2}$ must be zero, thus $\frac{ka}{2} = g\pi$ where $g = 0,1,2,3 \ldots$ etc. Finally if the toroid has a major radius R_T then $a = 2\pi R_T$ and this gives $k = \frac{g}{R_T}$ and from equation (14)

$$n = j\sqrt{\Gamma e^2 + \left(\frac{g}{R_T}\right)^2} .$$

The solution for E_y is then:

$$E_y = (A \text{ Sin } nx + B \text{ Cos } nx) \text{ Cos } kz \qquad \ldots (16)$$

Suppose $^{k}\gamma_e = \sqrt{\Gamma_e^2 + k^2}$ then $n = j\,^{k}\gamma_e$

Equation (16) can be rewritten as

$$E_y = (P \text{ Sinh } {}^{k}\gamma_e\, x + Q \text{ Cosh } {}^{k}\gamma_e\, x) \text{ Cos } kz \qquad \ldots (17)$$

where P and Q are new constants, and may of course be complex. Also from

equation (9)

$$H_z = - \frac{k\gamma_e}{j\omega\mu} (P \text{ Cosh } {}^{k}\gamma_e x + Q \text{ Sinh } {}^{k}\gamma_e x) \text{ Cos } kz \qquad \ldots (18)$$

and the electromagnetic field impedance ${}^{y}_{z}Z_e$ which is associated with propagation along OX is given by

$$\begin{aligned} {}^{y}_{z}Z_e &= \frac{E_y}{H_z} \\ &= - \frac{j\omega\mu}{{}^{k}\gamma_e} \frac{P \text{ Sinh } {}^{k}\gamma_e x + Q \text{ Cosh } {}^{k}\gamma_e x}{P \text{ Cosh } {}^{k}\gamma_e x + Q \text{ Sinh } {}^{k}\gamma_e x} \cdot \qquad \ldots (19) \end{aligned}$$

Note that this impedance is not a function of z so the modal propagation problem in the x direction is essentially one-dimensional. The value of the field impedance does however depend on the mode being considered, i.e. on the value of g and hence the value of k. It is convenient and appropriate in discussing the one dimensional modal problem to refer to ${}^{k}\gamma_e$ as the mode intrinsic propagation constant and $\frac{j\omega\mu}{{}^{k}\gamma_e}$ as the mode intrinsic field impedance ${}^{k}Z_{oe}$.

In terms of the problem parameters these are:

$${}^{k}\gamma_e = \sqrt{j\omega\mu \; j\omega\varepsilon + k^2} = \sqrt{j\omega\mu \; (j\omega\varepsilon + \frac{k^2}{j\omega\mu})},$$

and

$${}^{k}Z_{oe} = \sqrt{\frac{j\omega\mu}{j\omega\mu \; j\omega\varepsilon + k^2}} = \sqrt{\frac{j\omega\mu}{j\omega\varepsilon + \frac{k^2}{j\omega\mu}}} \cdot$$

Relating ${}^{k}\gamma_e$ and ${}^{k}Z_{oe}$ to the propagation constant and characteristic impedance of a one-dimensional electrical transmission line it is clear from the above expressions that the form of one elemental section of such an electrical analogue is as shown in Fig.6 where voltage is analogous to the electric field E_y and current analogous to the magnetic field H_z.

Using standard transmission line theory, the input impedance to such a line of length ℓ terminated in a short circuit, i.e. the vacuum in this case surrounded by an infinitely conducting metal wall, is given by:

$$ {}^{y}_{z}Z_{e} = {}^{k}Z_{oe} \tanh {}^{k}\gamma_{e} \ell \qquad \ldots (20) $$

At low frequencies $(\omega \to o)$ ${}^{k}\gamma_{e}$ approaches k and the impedance approaches $j\omega\mu L_e$ (an inductive reactance) where L_e is a constant dependent on the mode number under consideration. Thus $\frac{1}{{}^{\theta}_{z}Z^{+}_{e}}$ in the flow diagram of Fig.4 is equal to $\frac{1}{s\mu L_e}$ $(s = \frac{d}{dt} = j\omega$ in cissoidal analysis) and this has exactly the same form as $Z_n = \frac{K}{s}$ in the mass spring flow diagram of Fig.2(a).

A similar low frequency approximation can be obtained from an analysis of Z_e in cylindrical geometry but here the mathematics will involve Bessel functions[7]. If the fluid surface is at a radius r_o and the infinitely conducting wall has a radius R_o then the outward looking field impedance ${}^{\theta}_{z}Z^{+}_{e}$ is derived in Ref.8 Pt.II Appendix G3 equation G3.25 and is -

$$ {}^{\theta}_{z}Z^{+}_{e} = \frac{j\omega\mu}{k\gamma_e} \frac{I_1(k\gamma_e R_o)\, K_1(k\gamma_e r_o) - K_1(k\gamma_e R_o)\, I_1(k\gamma_e r_o)}{I_1(k\gamma_e R_o)\, K_o(k\gamma_e r_o) + K_1(k\gamma_e R_o)\, I_o(k\gamma_e r_o)} \qquad \ldots (21) $$

where I and K are the modified Bessel functions.

At low frequencies this also reduces to an expression of the form $j\omega\mu L_e$ (an inductive reactance) as was the case for Cartesian geometry.

3.3 The Acoustic Field Impedance ${}_{r}Z^{-}_{a}$

Since this impedance is related to hydrodynamic waves propagating into the body of the fluid, this aspect of the problem must be worked out in cylindrical geometry. The linearised acoustic wave equations are:

$$ \frac{1}{r} \frac{\partial(ru_r)}{\partial r} + \frac{\partial u_z}{\partial z} = \frac{-j\omega p}{\theta_o P_o} \qquad \ldots (22) $$

$$ \frac{\partial p}{\partial r} = -j\omega\rho_o u_r \qquad \ldots (23) $$

and

$$ \frac{\partial p}{\partial z} = -j\omega\rho_o u_z \,, \qquad \ldots (24) $$

where p_o = mean pressure, ρ_o = mean density, and θ_o = ratio of the specific

heats.

Eliminating u_r and u_z gives:

$$\frac{\partial^2 p}{\partial r^2} + \frac{1}{r}\frac{\partial p}{\partial r} + \frac{\partial^2 p}{\partial z^2} - \frac{(j\omega)^2 \rho_o p}{\theta_o p_o} = 0,$$

or

$$\frac{\partial^2 p}{\partial r} + \frac{1}{r}\frac{\partial p}{\partial r} + \frac{\partial^2 p}{\partial z^2} - \Gamma_a^2 p = 0 \ , \qquad \ldots (25)$$

where

$$\Gamma_a = j\omega \sqrt{\frac{\rho_o}{\theta_o p_o}}$$

is the intrinsic propagation constant for acoustic waves.

Assuming as before that $p = p(r)\, p(z)$ and separating the variables the solution of equation (25) is

$$p = \left[A\, I_o ({}^k\gamma_a r) + B\, K_o ({}^k\gamma_a r) \right] (C \sin kz + D \cos kz) \ , \qquad \ldots (26)$$

where

$${}^k\gamma_a = \sqrt{\Gamma_a^2 + k^2}$$

is the mode intrinsic propagation constant for acoustic waves.

From equation (22)

$$u_r = - \frac{{}^k\gamma_a}{j\omega\rho_o} \left[A\, I_1 ({}^k\gamma_a r) - B\, K_1 ({}^k\gamma_a r) \right] (C \sin kz + D \cos kz) \qquad \ldots (27)$$

and from equations (26) and (27) the acoustic field impedance ${}_r\bar{Z}_a$ looking radially into the fluid from the surface at radius r_o is

$${}_r\bar{Z}_a = \frac{p}{-u_r} = \frac{j\omega\rho_o}{{}^k\gamma_a} \frac{I_o({}^k\gamma_a r_o)}{I_1({}^k\gamma_a r_o)} \ . \qquad \ldots (28)$$

In equation (28) the term $\frac{j\omega\rho_o}{{}^k\gamma_a}$ is the mode intrinsic field impedance ${}^kZ_{oa}$ for acoustic waves.

At low frequencies $(\omega \to 0)$ corresponding to incompressible fluid flow the acoustic field impedance ${}_r\bar{Z}_a$ approximates to $j\omega\rho_o G_a$ where G_a is a constant

depending on the mode number. Thus as before $\frac{1}{{}_{r}Z_{a}^{-}}$ in the flow diagram of Fig.4 is equal to $\frac{1}{s\rho_o G_a}$ and this has the same form as $\frac{1}{Z_m} = \frac{1}{sM}$ in the mass-spring flow diagram of Fig.2(a)

3.4 Stability

The stability of this simple θ-pinch MHD system can now be studied by considering the roots of equation (7) since the field impedance ${}_{\theta}^{z}Z_{e}^{+}$ and ${}_{r}Z_{a}^{-}$ have been determined. At low frequencies the dispersion relationship becomes:

$$1 + \frac{B_{oz}^2}{s^2 \mu \rho_o G_a L_e} = 0 , \qquad \ldots (29)$$

and

$$s^2 = - \frac{B_{oz}^2}{\mu \rho_o G_a L_e} \qquad \ldots (30)$$

The system is therefore neutrally stable.

This can also be seen from the flow diagram of Fig.4 with the low frequency approximation $s\mu L_e$ and $s\rho_o G_a$ inserted for ${}_{\theta}^{z}Z_{e}^{+}$ and ${}_{r}Z_{a}^{-}$ respectively. The form of the flow diagram is then identical with that of the mass-spring model in Fig.2(a) (a closed loop containing two integrators and a phase inverter) and as such is neutrally stable.

At high frequencies it is much more difficult, if not impossible, to determine the roots of the dispersion relationship analytically. However, if numerical values of the system parameters are known, the open loop Nyquist diagram can be drawn and the stability of the system inferred from the position of the point (-1,0) on the diagram; this has to be done for each mode.

If the bounding wall has finite conductivity the effect of this on the stability can be deduced from the equivalent electrical line in Fig.6. This results in a resistive termination, so at low frequencies the line input impedance ${}_{z}^{y}Z_{e}$ takes the form $R + j\omega L$. This form applies for all mode numbers, but the resistive component relative to the inductive component at any frequency gets less as

the mode number increases.

With a termination of this type the dispersion relationship, equation (7) becomes:

$$1 + \frac{B_{oz}^2}{(R + sL)\, s\rho_o G_a} = 0 \qquad \ldots (31)$$

giving on solution

$$s = -\frac{R}{2L} \pm \sqrt{\frac{R^2}{4L^2} - \frac{B_{oz}^2}{\rho_o G_a L}} \qquad \ldots (32)$$

Both roots have a negative real part so the system is stable and additionally will damp out any small injected disturbance. This example indicates a way in which the impedance of the power supply can affect the stability of the fluid.

4. STABILITY OF THE SIMPLE Z-PINCH CONFIGURATION

This section considers the stability of a cylinder of infinitely conducting fluid, carrying an axial surface current of J_{oz} amps per metre of circumference, enclosed within an infinitely conducting cylindrical metal wall. The surface current J_{oz} will have associated with it a circumferential magnetic field in the vacuum outside the fluid of magnitude $H_{o\theta}\frac{r_o}{r}$ where $H_{o\theta} = J_{oz}$. As before, attention will be confined to a two dimensional model with variations along the axis and radius only.

4.1 The Closed Loop Flow Diagram

The system is postulated to be initially in static equilibrium where the fluid pressure P_o is again balanced by the surface magnetic pressure $\frac{\mu H_{o\theta}^2}{2}$. If the surface of the fluid is disturbed and moves sinusoidally about its equilibrium position with a radial component of velocity u_r and an axial component of velocity u_z, then as before the fluctuating surface pressure p is related to u_r by $-u_r = \frac{p}{r\bar{Z}_a}$ where $r\bar{Z}_a$ is the same acoustic field impedance, looking radially into the fluid, as was discussed in Section 3.3. The fluid surface moving with velocities u_r and u_z then interacts with the steady magnetic field $H_{o\theta}$

producing induced fluctuating electric fields on the surface in the z and r directions.

As before, because of the infinite conductivity of the fluid, these induced fields are balanced by fluctuating components E_z and E_r and they in turn give rise to a fluctuating magnetic field H_θ associated with electromagnetic wave propagation in the radial and axial directions. In the radial direction E_z is related to H_θ by $-H_\theta = \frac{E_z}{{}_{\theta}Z_e^{z+}}$ where ${}_{\theta}Z_e^{z+}$ is the electromagnetic field impedance looking radially outwards from the fluid surface into the vacuum. ${}_{\theta}Z_e^{z+}$ is not the same impedance as was discussed in Section 3.2 because here the radial propagation is due to E_z and H_θ whereas before it was due to E_θ and H_z. As before however the two dimensional nature of the problem is implicit in ${}_{\theta}Z_e^{z+}$.

Finally, the steady current J_{oz} flowing on the surface of the fluid reacts with the fluctuating magnetic field H_θ producing a surface pressure and this completes the loop. Unlike the θ-pinch problem however this is not the whole story, because the decrease in the vacuum magnetic field as one moves radially away from the fluid surface leads to a further component of fluctuating pressure which can be represented as an additional loop in the flow diagram.

This extra pressure fluctuation, arising from the displacement of the fluid in a non-uniform magnetic field will be referred to as the displacement term and is calculated as follows:

Magnetic pressure at radius r outside the fluid

$$= \frac{\mu H_{o\theta}^2 \, r_o^2}{2r^2} \qquad \ldots (33)$$

$\therefore$ Pressure gradient $\dfrac{\partial p}{\partial r} = \dfrac{-\mu H_{o\theta}^2 \, r_o^2}{r^3}$ $\qquad \ldots (34)$

$$= \frac{-\mu H_{o\theta}^2}{r_o} \quad \text{at the surface radius } r_o.$$

Fluid surface radial velocity $= u_r$,

$\therefore$ Surface radial displacement $= \dfrac{u_r}{s}$.

Hence fluctuating surface pressure = pressure change/unit displacement $(\frac{\partial p}{\partial r})$ × displacement $(\frac{u_r}{s})$

$$= \frac{-\mu H_{o\theta}^2}{r_o} \frac{u_r}{s} \qquad \ldots (35)$$

The closed loop flow diagram, including this displacement term, is shown in Fig.7.

The open loop transfer function is

$$A(s) = \frac{-\mu^2 J_{oz} H_{o\theta}}{r\bar{Z}_a \, {}_{\theta}Z_e^+} + \frac{\mu H_{o\theta}^2}{s_r \bar{Z}_a \, r_o} ,$$

$$= - \frac{B_{o\theta}^2}{r\bar{Z}_a \, {}_{\theta}Z_e^+} + \frac{B_{o\theta}^2}{s\mu_r \bar{Z}_a \, r_o} \qquad \ldots (36)$$

and the dispersion relationship $1 - A(s) = 0$ becomes

$$1 + \frac{B_{o\theta}^2}{r\bar{Z}_a \, {}_{\theta}Z_e^+} - \frac{B_{o\theta}^2}{s\mu_r \bar{Z}_a \, r_o} = 0 \qquad \ldots (37)$$

As before, the system stability depends on the roots of this equation. At low frequencies ${}_r\bar{Z}_a$ is again equal to $s\rho_o G_a$ but the form of ${}_{\theta}Z_e^+$ is not yet known. It is interesting to note that if ${}_{\theta}Z_e^+$ is assumed to be infinite, then the dispersion relationship reduces to

$$1 - \frac{B_{o\theta}^2}{s^2 \mu \rho_o G_a r_o} = 0 \qquad \ldots (38)$$

giving on solution a positive value for s. If the electromagnetic field impedance is infinite then the displacement term causes instability. This is also clear from the flow diagram, Fig.7, because the upper loop, corresponding to the displacement term, consists of two integrators in cascade only, and is exactly analogous to the mass-spring flow diagram, Fig.2(a), where the spring constant is negative. The behaviour of the complete system however, depends on the form of ${}_{\theta}Z_e^+$ which is studied in the next section.

4.2 The Electromagnetic Field Impedance $^{z}_{\theta}Z^{+}_{e}$

Assuming the vacuum annular space between the fluid and the conducting wall is thin, then as in Section 3.2 it is simpler to evaluate $^{z}_{\theta}Z^{+}_{e}$ in Cartesian geometry where E_r and H_θ become E_x and H_y respectively. Consider a section through the vacuum space, between the fluid and the wall, as shown in Fig.8. The electromagnetic field equations are:

$$\frac{\partial H_y}{\partial z} = - j\omega\varepsilon E_x \qquad \ldots (39)$$

$$\frac{\partial H_y}{\partial x} = j\omega\varepsilon E_z \qquad \ldots (40)$$

and

$$\frac{\partial E_x}{\partial z} - \frac{\partial E_z}{\partial x} = - j\omega\mu H_y \qquad \ldots (41)$$

From equations (39), (40) and (41) may be obtained:

$$\frac{\partial^2 H_y}{\partial x^2} + \frac{\partial^2 H_y}{\partial z^2} = \Gamma_e^2 H_y \qquad \ldots (42)$$

where

$$\Gamma_e^2 = j\omega\varepsilon j\omega\mu$$

Equation (42) can be solved exactly as equation (11) in Section 3.2 giving:

$$H_y = (P \text{ Sinh } {}^{k}\gamma_e x + Q \text{ Cosh } {}^{k}\gamma_e x) \text{ Cos } kz \ , \qquad \ldots (43)$$

where

$${}^{k}\gamma_e = \sqrt{\Gamma_e^2 + k^2}$$

and

$$k = \frac{2\pi g}{a} \ , \ (g = 0, 1, 2, 3 \ldots \text{ etc.})$$

$$= \frac{g}{R_r} \quad \text{for a toroidal arrangement.}$$

From equation (40)

$$E_z = \frac{{}^{k}\gamma_e}{j\omega\varepsilon} (P \text{ Cosh } {}^{k}\gamma_e x + Q \text{ Sinh } {}^{k}\gamma_e x) \text{ Cos } kz \qquad \ldots (44)$$

and the electromagnetic field impedance ${}^{z}_{y}Z_{e}$ which governs propagation along ox is given by:

$$
\begin{aligned}
{}^{z}_{y}Z_{e} &= -\frac{E_z}{H_y} \\
&= -\frac{{}^{k}\gamma_{e}}{j\omega\varepsilon}\ \frac{P \operatorname{Cosh} {}^{k}\gamma_{e}\, x + Q \operatorname{Sinh} {}^{k}\gamma_{e}\, x}{P \operatorname{Sinh} {}^{k}\gamma_{e}\, x + Q \operatorname{Cosh} {}^{k}\gamma_{e}\, x} \qquad \ldots (45)
\end{aligned}
$$

As before ${}^{k}\gamma_{e}$ is the mode intrinsic propagation constant and $\frac{{}^{k}\gamma_{e}}{j\omega\varepsilon}$ is the mode intrinsic field impedance ${}^{k}Z_{oe}$.

In terms of the system parameters these are:

$${}^{k}\gamma_{e} = \sqrt{j\omega\varepsilon\, j\omega\mu + k^2} = \sqrt{\left(j\omega\mu + \frac{k^2}{j\omega\varepsilon}\right) j\omega\varepsilon}\ ,$$

and

$${}^{k}Z_{oe} = \sqrt{\frac{j\omega\varepsilon\, j\omega\mu + k^2}{j\omega\varepsilon}} = \sqrt{\frac{\left(j\omega\mu + \frac{k^2}{j\omega\varepsilon}\right)}{j\omega\varepsilon}}\ ,$$

and from these expressions for ${}^{k}\gamma_{e}$ and ${}^{k}Z_{oe}$ it is clear that one elemental section of the equivalent electrical transmission line is as shown in Fig.9.

4.3 Stability

Continuing in Cartesian geometry, the impedance looking into a transmission line of the type shown in Fig.9, of length ℓ and terminated in a short circuit is:

$${}^{z}_{y}Z_{e} = {}^{k}Z_{oe} \tanh {}^{k}\gamma_{e}\, \ell \qquad \ldots (46)$$

At low frequencies $(\omega \to 0)$ the propagation constant ${}^{k}\gamma_{e}$ approaches k and the impedance approaches $\frac{S_e}{j\omega\varepsilon}$ (a capacitive reactance) where S_e is a constant depending on the mode number. The cylindrical solution for ${}^{z}_{\theta}Z^{+}_{e}$ is derived in Reference 8, Pt. II, Appendix G Equation G1.20, and is:

$${}^{z}_{\theta}Z^{+}_{e} = \frac{{}^{k}\gamma_{e}}{j\omega\varepsilon}\ \frac{I_o({}^{k}\gamma_{e}R_o)\, K_o({}^{k}\gamma_{e}r_o) - K_o({}^{k}\gamma_{e}R_o)\, I_o({}^{k}\gamma_{e}r_o)}{I_o({}^{k}\gamma_{e}R_o)\, K_1({}^{k}\gamma_{e}r_o) + K_o({}^{k}\gamma_{e}R_o)\, I_1({}^{k}\gamma_{e}r_o)} \qquad \ldots (47)$$

As in the Cartesian geometry case at low frequencies, this also reduces to an expression of the form $\frac{S_e}{j\omega\varepsilon}$ (a capacitive reactance). The dispersion

relationship, equation (37) therefore becomes:

$$1 + \frac{B_{o\theta}^2 \varepsilon}{\rho_o S_e G_a} - \frac{B_{o\theta}^2}{s^2 \mu \rho_o G_a r_o} = 0 \qquad \ldots (48)$$

$$s^2 \left[1 + \frac{B_{o\theta}^2 \varepsilon}{\rho_o S_e G_a} \right] = \frac{B_{o\theta}^2}{\mu \rho_o G_a r_o} \qquad \ldots (49)$$

One root is always positive and the system is unstable.

A method of improving the stability of this simple z pinch is to immerse the fluid in a z-directed magnetic field. This field is usually established in z-pinch plasma experiments before the pinch or collapse phase, when the plasma conductivity is low. During the collapse phase, the z field is trapped in the plasma and increases in magnitude as the radius falls. This phase ends when the trapped field reaches a value H_{oz} such that the pressure balance relationship

$$p_o + \frac{\mu H_{oz}^2}{2} = \frac{\mu H_{o\theta}^2}{2}$$

is satisfied.

Consider then the idealised situation of a cylindrical fluid of low bulk conductivity but having an infinitesimally thin surface layer of infinite conductivity, carrying an external surface current of J_{oz} amps. per metre of circumference. Associated with this current will be a θ-directed magnetic field in the vacuum space outside the fluid of magnitude $\frac{H_{o\theta} r_o}{r}$ where $H_{o\theta} = J_{oz}$. In addition, there is a z-directed magnetic field of magnitude H_{oz} trapped in the low conductivity fluid and unable to escape because of the infinitely conducting surface layer. This will of necessity give rise to an internal surface current of $J_{o\theta}$ amp. per metre of axial length where $H_{oz} = J_{o\theta}$. The assumption of a low conductivity fluid inside the surface layer simplifies the problem, in that the acoustic and electromagnetic waves propagating through the fluid are not coupled along the radius (as in Reference 8, Part I, Section I, Fig.4) but are coupled only at the surface r_o.

The flow diagram for this arrangement is identical with Fig.7 but with an

extra loop, corresponding to electromagnetic wave propagation through the fluid from the surface inwards towards the centre. This is shown in Fig.10. The field impedance involved in this loop is ${}^{\theta}_{z}Z^{-}_{e}$. This inward looking electromagnetic field impedance (which here must be in cylindrical co-ordinates) is derived in Reference 8, Part 2, Appendix G3, Equation G3.8 and is:

$$ {}^{\theta}_{z}Z^{-}_{e} = \frac{j\omega\mu}{k\gamma_e} \frac{I_1(k\gamma_e r_o)}{I_o(k\gamma_e r_o)} \qquad \ldots (50) $$

At low frequencies and low mode numbers, using the approximations given in Reference 9, Appendix 2 when $k\gamma_e r_o$ approaches 0 this becomes:

$$ {}^{\theta}_{z}Z^{-}_{e} = \frac{j\omega\mu}{k\gamma_e} \frac{k\gamma_e r_o}{2} $$

$$ = \frac{j\omega\mu r_o}{2} \qquad \ldots (51) $$

The open loop transfer function for Fig.10 is:

$$ A(s) = -\frac{B^2_{o\theta}}{r Z^{-}_{a}\ {}^{z}Z^{+}_{e}} + \frac{B^2_{o\theta}}{s\mu_r Z^{-}_{a}\ r_o} - \frac{B^2_{oz}}{r Z^{-}_{a}\ {}^{\theta}Z^{-}_{e}} \qquad \ldots (52) $$

and the dispersion relationship $1 - A(s) = 0$ becomes:

$$ s^2 \left[1 + \frac{B^2_{o\theta}\ \varepsilon}{\rho_o S_e G_a} \right] = \frac{B^2_{o\theta}}{\mu\rho_o G_a r_o} - \frac{2\ B^2_{oz}}{\mu\rho_o G_a r_o} \qquad \ldots (53) $$

$$ = \frac{B^2_{o\theta}}{\mu\rho_o G_a r_o} \left[1 - \frac{2\ B^2_{oz}}{B^2_{o\theta}} \right] . \qquad \ldots (54) $$

This is stable if

$$ \frac{B^2_{oz}}{B^2_{o\theta}} > \frac{1}{2} \qquad \ldots (55) $$

For higher mode numbers in equation (50) it can be shown from the Bessel function expansions[7] that

$$ \frac{I_1\ (k\gamma_e r_o)}{I_o\ (k\gamma_e r_o)} \ , $$

is always less than $\frac{k_\gamma r_o}{2}$; thus equation (55) defines a condition for the prevention of sausage-type instabilities in the idealised two-dimensional z-pinch which is applicable to all mode numbers.

Attention has been confined, in this paper, to two-dimensional systems, but the same techniques can be equally well applied to the response of wave and diffusion-like systems in three dimensions and an example of this is given in Reference 8, Part I, Section 6.

It is interesting also to note that in equation (52) the positive term on the right-hand side which could bring about instability stems from the displacement term due to a negative magnetic field gradient outside the fluid. If this gradient were positive, corresponding to the magnetic field increasing away from the fluid surface, this term would change sign and the system would become unconditionally stable.

5. CONCLUSIONS

The paper has shown how the engineering concepts of transfer functions and flow diagrams, generally used to determine the stability of closed loop lumped parameter dynamic systems, can be applied to a study of the stability of an infinitely conducting fluid immersed in a magnetic field.

The authors feel that the conversion of the magnetohydrodynamic system to an electrical analogue, or equivalent circuit, will help considerably the control engineer to get a better physical understanding of the problem. For example, the paper shows clearly how the very complicated expressions like equations (21) and (47) which occur in analytical studies of magneto-fluid-stability have very simple physical interpretations in terms of field impedance.

It is believed that an extension of these techniques might be applied advantageously of fluids having finite conductivity and to geometrical configurations other than the θ and Z pinches considered in the paper.

It is likely that this approach is also applicable to a variety of physical systems where wave and diffusion processes are involved.

6. REFERENCES

1. BOOKER, H.G. The elements of wave propagation using the impedance concept. J. Inst. Elec. Eng., 1947, 94, pt.3, p.171.

2. SCHELKUNOFF, S.A. Electromagnetic waves. Princeton, Van Nostrand, 1943.

3. NYQUIST, H. Regeneration theory. Bell Sys. Tech. J., 1932, 11, p.126.

4. TRUXHALL, J.G. Automatic feedback control system synthesis. New York, McGraw Hill, 1955.

5. CUNNINGHAM, W.J. Introduction to non-linear analysis. New York, McGraw Hill, 1958.

6. TAYLER, R.J. Hydromagnetic instabilities of a cylindrical gas discharge. London, H.M.S.O., 1958. AERE-TP/R 2374.

7. McLACHLAN, N.W. Bessel functions for engineers. 2nd ed. Oxford, Clarendon Press, 1955.

8. COOPER, W.H.B. and others. The engineering concepts of equivalent networks, transfer functions and field impedance in magnetohydrodynamics. (Three parts). Harwell, Atomic Energy Research Establishment, 1963. AERE-M 1213.

9. COOPER, W.H.B. Diffusion of electricity. Electron Tech., 1962, 39, p.279.

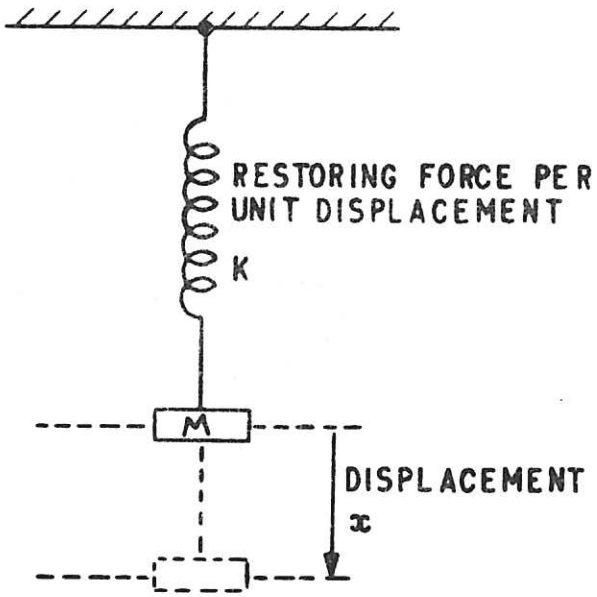

Fig. 1 The mass-spring model (CLM-P69)

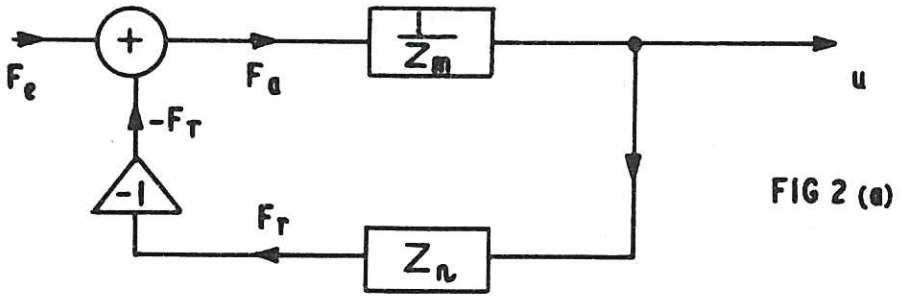

Fig. 2(a) (CLM-P69)
Transfer function flow diagram for the mass-spring model

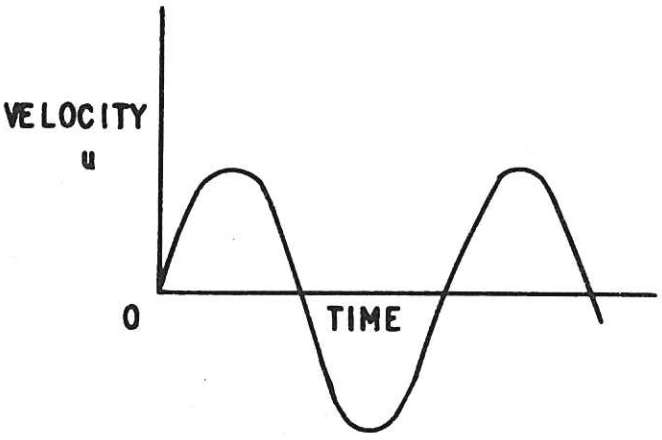

Fig. 2(b) (CLM-P69)
Velocity time graph for the mass-spring model with a positive spring constant

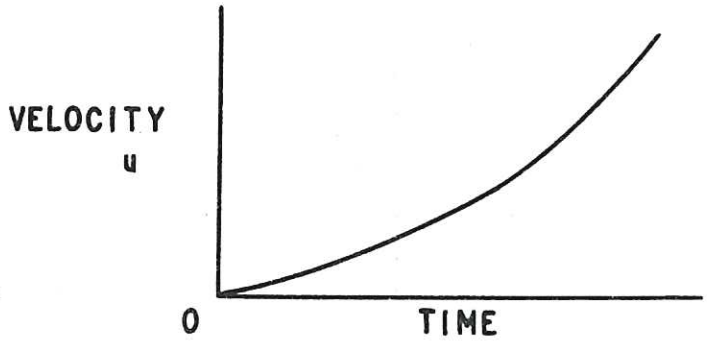

Fig. 2(c) (CLM-P69)
Velocity time graph for the mass-spring model with a negative spring constant

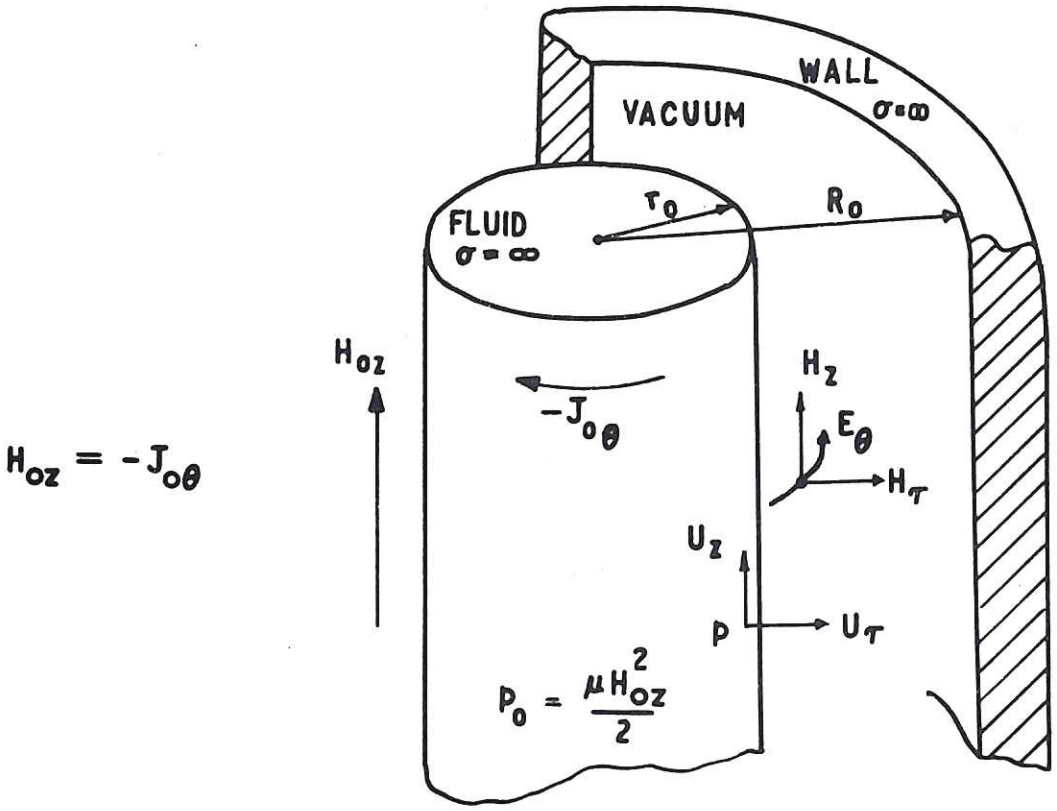

Fig. 3 Schematic of a two-dimensional θ-pinch experiment (CLM-P69)

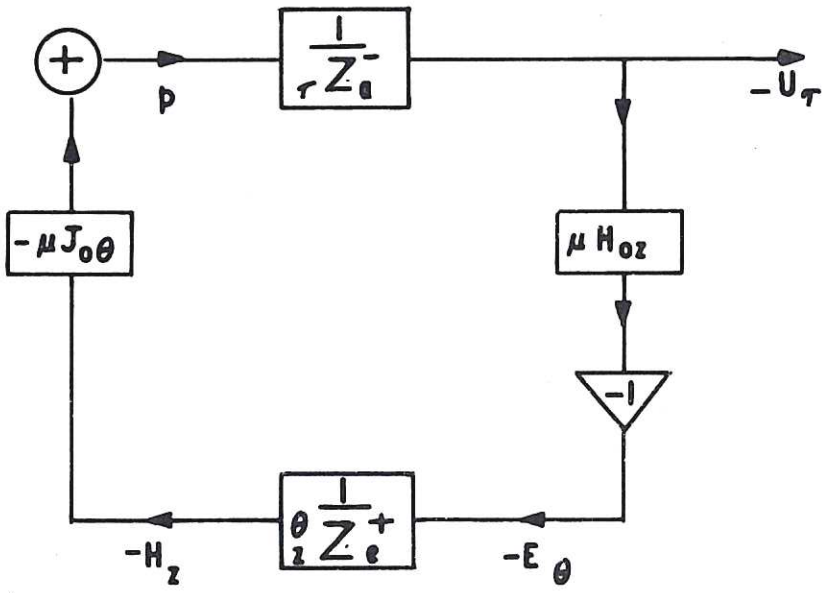

Fig. 4 (CLM-P69)
Transfer function flow diagram for the θ-pinch

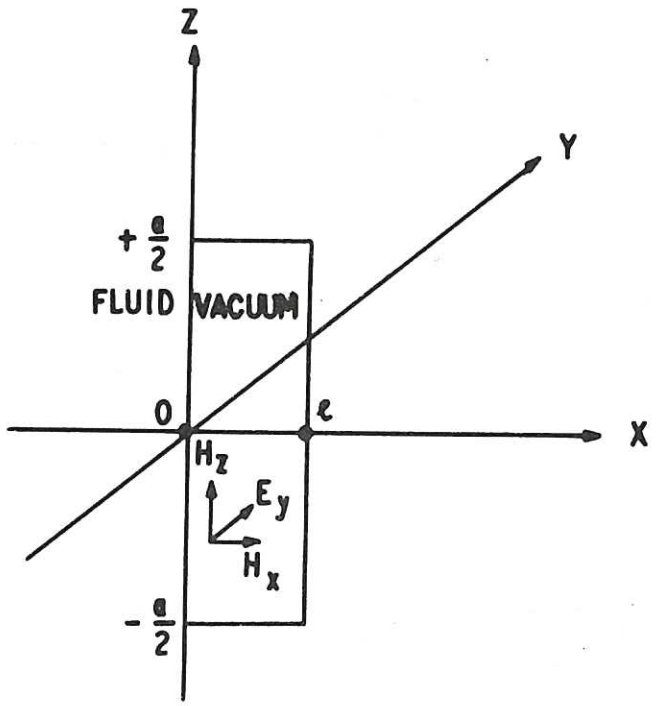

Fig. 5 (CLM-P 69)
Cartesian representation of a radial section through the vacuum space of the θ-pinch configuration

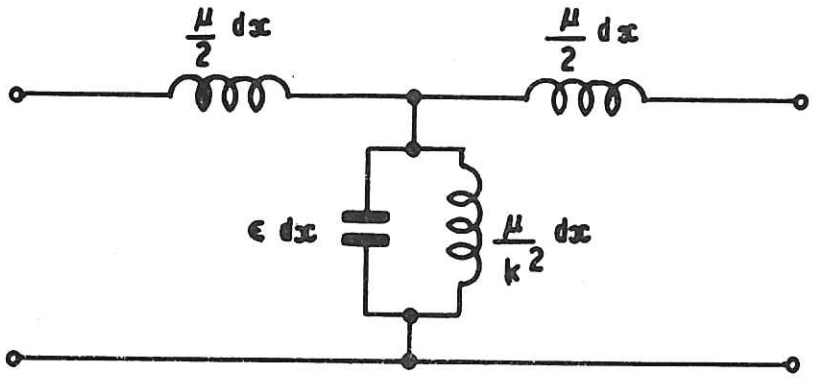

Fig. 6 (CLM-P 69)
An elemental section of the transmission line analogue of the vacuum space in the θ-pinch

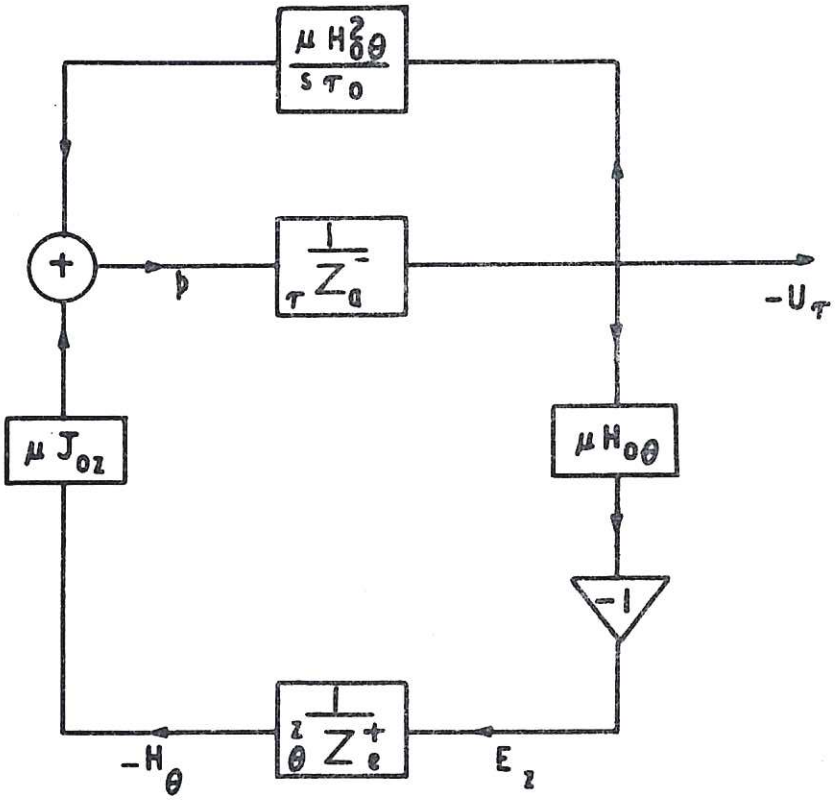

Fig. 7 (CLM-P 69)
Transfer function flow diagram for the z-pinch

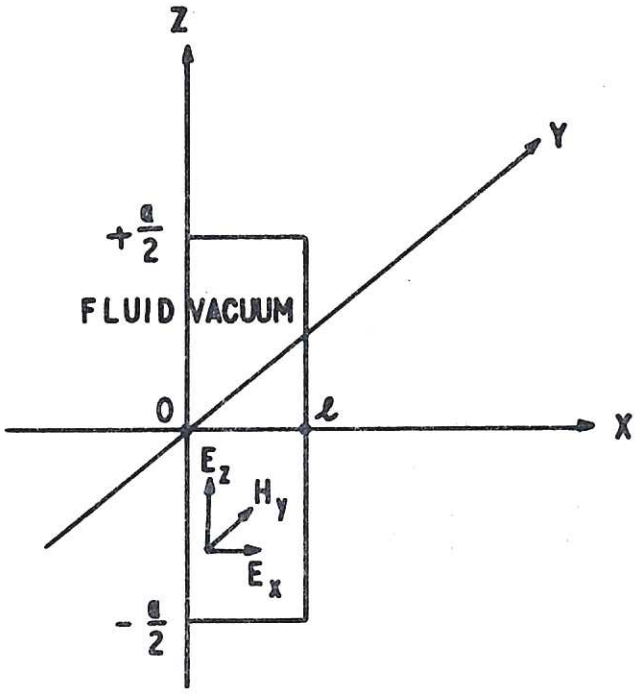

Fig. 8 (CLM-P 69)
Cartesian representation of radial section through the vacuum space of the z-pinch configuration

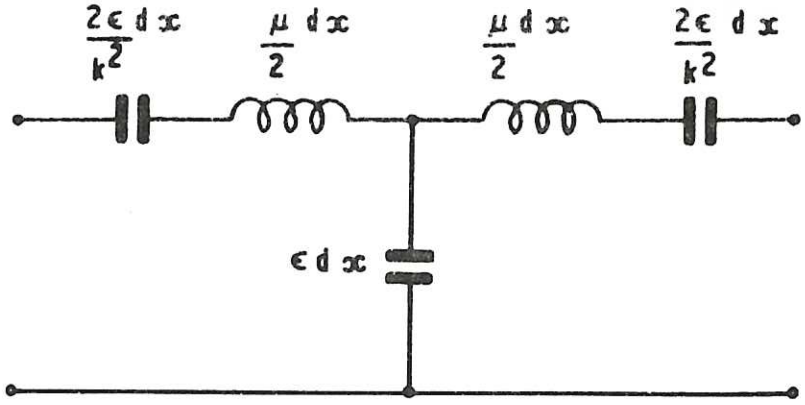

Fig. 9 (CLM-P 69)
An elemental section of the transmission line analogue of the vacuum space in the z-pinch

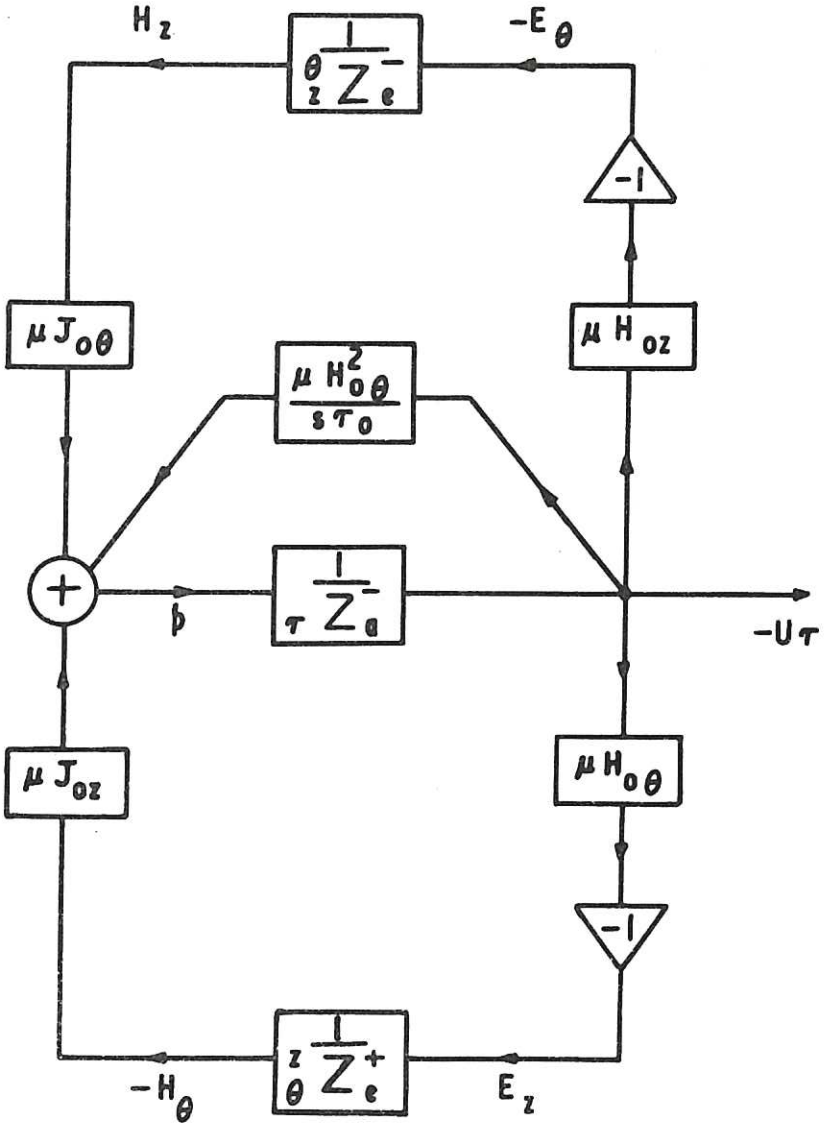

Fig. 10 (CLM-P 69)
Transfer function flow diagram for the z-pinch with a stabilising axial magnetic field